

Numerical Simulation of Double Diffusive Laminar Mixed Convection in a Horizontal Rotating Annulus

Part (II): Effect of Prandtl number and buoyancy ratio

Medhat M. Sorour¹, Mohamed A. Teamah², Wael M. El-Maghlany^{1C}, Heba M. Abdel Aziz³

¹Mechanical Engineering Department, Alexandria University, Alexandria, EGYPT

²Arab Academy for Science, Technology and Maritime Transport, Alexandria, EGYPT

³Alexandria Higher Institute for Engineering and Technology, Alexandria, EGYPT

Received: 15/08/2013 – Revised 22/04/2014 – Accepted 19/05/2014

Abstract

A numerical study of double-diffusive mixed convection within a horizontal rotating annulus has been investigated. The outer cylinder is fixed but the inner cylinder is considered to rotate in clockwise and anti-clockwise directions to introduce the forced convection effect. In addition, the solutal and thermal buoyancy forces are sustained by maintaining the inner and outer cylinder at uniform temperatures and concentrations but their values for the inner are higher than the outer. The flow is considered laminar regime under steady state conditions. The transport equations for the continuity, momentum, energy and mass transfer are solved using the finite volume technique. The considered domains in this investigation are: $-15 \leq N \leq 15$, $0.01 \leq Ri \leq 100$ and $0.01 \leq Pr \leq 100$. While the thermal Grashof number, Lewis number and the radius ratio are kept constant at values equal to 10^4 , 1 and 2 respectively. The effect of the selected parameters on the local and average Nusselt and Sherwood numbers are presented and studied. Finally, this investigation concerned with selection the best direction of the inner cylinder rotation to enhance both heat and mass transfer. A comparison was made with the published results and a good agreement was found.

Keywords: Double diffusive flow; Rotating annulus; Mixed convection; Numerical simulation

1. Introduction

Double-diffusive convection is an important fluid dynamics topic that describes a form of convection driven by two different density gradients which have different rates of diffusion. Convection in fluids is driven by density variation within them.

These density variations may be caused by gradients in the composition of the fluid, or by differences in temperature (through thermal expansion). A series of numerical studies for the natural and mixed convection heat transfer in a horizontal rotating annulus were conducted by Joo-Sik Yoo [1-3], these studies cover a wide range of Grashof number, Prandtl number and the radius

^C Corresponding Author: Wael M. El-Maghlany

Email: elmaghlany@yahoo.com Telephone: +201223741891

© 2014 All rights reserved. ISSR Journals

Fax: +2035921853

PII: S2180-1363(14)6081-X

ratio. In addition, several studies were reported on the natural convection heat transfer in a horizontal annulus. Jiro et al. [4] studied the effect of the thermal Rayleigh number and the radius ratio on the thermal and hydrodynamic instabilities for air filled annuli. Alawadhi [5] investigated numerically the natural convection flow in a horizontal annulus enclosure with a transversely oscillating inner cylinder, the study showed that the oscillating frequency of the inner cylinder has a significant effect on the average Nusselt number at the inner cylinder but it had an insignificant effect on the average Nusselt number at the outer cylinder. Desia and Vafait [6] investigated the natural convection in a horizontal, annular cavity which communicates with the surroundings through its open end experimentally and numerically. An additional numerical study on the mixed convection heat transfer for non-Newtonian fluid between two coaxial rotating cylinders was investigated for Prandtl number equals to 5 by Amoura et al. [7], the effects of different parameters on the heat transfer and the fluid flow were examined. For the double diffusion mixed convection problems, Amiri and Khanafer [8] carried out a numerical investigation of double diffusive mixed convection in a horizontal annulus with rotating outer cylinder, the inner cylinder was maintained at a uniform but higher concentration and temperature values, they studied the effect of different parameters on the heat and mass transfer. Comprehensive reviews on the study of double diffusive laminar mixed convection in a horizontal annulus with hot, solutal and rotating inner cylinder were presented by Teamah [9]. In addition, Lee et al [10] investigated experimentally the double diffusive convection phenomena of a stably stratified salt- water solution due to lateral heating in a stationary and rotating annulus. Marcoux et al. [11] carried out an analytical and numerical study of double diffusive natural convection through a fluid saturated, vertical and homogeneous porous annulus subjected to uniform fluxes of heat and mass from the side. Khanafer et al. [12] studied a numerical investigation of natural convection heat transfer within a two-dimensional, horizontal annulus that is partially filled with a fluid-saturated porous medium; the working fluid was air while copper was used to represent the solid phase. From another view, Kenjeres and Hanjalid [13] investigated the natural convection in horizontal concentric and eccentric annuli with heated inner cylinder. Rahnema and Farhadi [14] studied turbulent natural convection between two horizontal concentric cylinders in the presence of radial fins numerically. From the previous review, the double diffusion mixed convection in a rotating annulus is very important in many engineering applications and it has a shortage in publications. Therefore, the present investigation is devoted to study this configuration.

2. Mathematical model

Two long concentric horizontal cylinders with gap width, b , are considered. The geometry of the problem is shown in Fig. 1. Both of the two cylinders are held at constant but different temperatures and concentrations of T_i, C_i and T_o, C_o ($T_i > T_o$) and ($C_i > C_o$). The temperature gradient generates the natural thermal diffusive force and the concentration gradient generates the natural solutal diffusive force. The inner cylinder is considered able to rotate in clockwise and anti-clockwise directions to create the forced convection. In addition, the flow in the annular region is assumed to be Newtonian, two-dimensional, steady and laminar. Also, all thermo-physical properties of the fluid are taken to be constant except for the density variation in the buoyancy term, where the Boussinesq approximation is considered to be linearly proportional to both temperature and concentration such that:

$$\rho = \rho_o [1 - \beta_T (T - T_o) - \beta_C (C - C_o)] \quad (1)$$

Where β_T and β_C are the coefficients for thermal and concentration expansions, respectively such that:

$$\beta_T = -\frac{1}{\rho_o} \left(\frac{\partial \rho}{\partial T} \right)_{p,C} \quad \text{and} \quad \beta_C = -\frac{1}{\rho_o} \left(\frac{\partial \rho}{\partial C} \right)_{p,T} \quad (2)$$

To put the governing equations in the dimensionless form, the following dimensionless variables are introduced to the governing equations.

$$V_r = \frac{v_r}{r_i}, V_\theta = \frac{v_\theta}{r_i}, R = \frac{r}{b}, \theta = \left(\frac{T - T_o}{T_i - T_o} \right), P' = \frac{p}{(\rho r_i)^2}, C' = \left(\frac{C - C_o}{C_i - C_o} \right) \quad (3)$$

The dimensionless form of governing equations for the continuity, momentum, thermal energy and species transport in the cylindrical coordinate are:

$$\left(\frac{\partial V_r}{\partial R} + \frac{V_r}{R} + \frac{\partial V_\theta}{R \partial \theta} \right) = 0 \quad (4)$$

$$\left(V_r \frac{\partial V_r}{\partial R} + V_\theta \frac{\partial V_r}{R \partial \theta} - \frac{V_\theta^2}{R} \right) = -\frac{\partial P'}{\partial R} - \frac{Gr_T}{Re^2} \left((1 + NC') \cos \theta \right) + \frac{1}{Re} \left(\frac{\partial^2 V_r}{\partial R^2} + \frac{1}{R} \frac{\partial V_r}{\partial R} - \frac{V_r}{R^2} + \frac{\partial^2 V_r}{R^2 \partial \theta^2} - \frac{2}{R^2} \frac{\partial V_\theta}{\partial \theta} \right) \quad (5)$$

$$\left(V_r \frac{\partial V_\theta}{\partial R} + V_\theta \frac{\partial V_\theta}{R \partial \theta} + \frac{V_r V_\theta}{R} \right) = -\frac{\partial P'}{R \partial \theta} + \frac{Gr_T}{Re^2} \left((1 + NC') \sin \theta \right) + \frac{1}{Re} \left(\frac{\partial^2 V_\theta}{\partial R^2} + \frac{1}{R} \frac{\partial V_\theta}{\partial R} - \frac{V_\theta}{R^2} + \frac{\partial^2 V_\theta}{R^2 \partial \theta^2} + \frac{2}{R^2} \frac{\partial V_r}{\partial \theta} \right) \quad (6)$$

$$\left(V_r \frac{\partial}{\partial R} + V_\theta \frac{\partial}{R \partial \theta} \right) = \frac{1}{Re Pr} \left[\frac{1}{R} \frac{\partial}{\partial R} \left(R \frac{\partial}{\partial R} \right) + \frac{\partial^2}{R^2 \partial \theta^2} \right] \quad (7)$$

$$\left(V_r \frac{\partial C'}{\partial R} + V_\theta \frac{\partial C'}{R \partial \theta} \right) = \frac{1}{Re Sc} \left[\frac{1}{R} \frac{\partial}{\partial R} \left(R \frac{\partial C'}{\partial R} \right) + \frac{\partial^2 C'}{R^2 \partial \theta^2} \right] \quad (8)$$

Where V_r , V_θ are the dimensionless velocity components in the radial and angular directions respectively, P' is the dimensionless pressure. $Re = r_i b / \nu$, is the rotational Reynolds number, $N = Gr_S / Gr_T$ is the Buoyancy ratio, $Sc = \nu / D$ is the Schmidt number, $Pr = \nu / \alpha$ is the Prandtl number. Whereas $Gr_S = g (c_i - c_o) b^3 / \nu^2$ and $Gr_T = g (T_i - T_o) b^3 / \nu^2$ are the solutal and thermal Grashof numbers.

For the boundary conditions, the temperature and concentration gradients are maintained by considering higher magnitudes at the inner cylinder. In addition, the outer cylinder is fixed but the inner cylinder is assumed to rotate in clockwise and anti-clockwise directions.

The dimensionless boundary conditions for the anti-clockwise and clockwise rotations are:

$$V_\theta = \pm 1, V_r = 0, \theta = 1.0 \text{ and } C' = 1.0, \text{ at } R = R_i \quad (9)$$

$$V_\theta = 0, V_r = 0, \theta = 0 \text{ and } C' = 0, \text{ at } R = R_o \quad (10)$$

The positive sign refers to the anti-clockwise rotation where the negative sign refers to the clockwise rotation. By defining the Nusselt number as the ratio between the actual heat transfer rate and the heat transferred by pure conduction, then the local Nusselt number along the inner cylinder is calculated as:

$$Nu_\theta = - \left(R \frac{\partial \theta / \partial R} {Nu_{cond}} \right)_{R=R_i} \quad (11)$$

Where Nu_{cond} is the Nusselt number in the case of heat transfer through the annulus by pure conduction and given by:

$$Nu_{cond} = \left(1 / \ln \frac{R_o}{R_i} \right) \quad (12)$$

From equations (13) and (14), the final form of the local Nusselt number is as follows:

$$Nu_\theta = \ln \left(\frac{R_i}{R_o} \right) \times \left(R \frac{\partial \theta}{\partial R} \right)_{R=R_i} \quad (13)$$

The average Nusselt number is calculated from integrating the local value over the circumference of the inner cylinder as follows:

$$Nu = \frac{1}{2f} \int_0^{2f} Nu_{\zeta} d\zeta. \quad (14)$$

Similarly, we can calculate both local and average Sherwood numbers as follows:

$$Sh_{\zeta} = \ln\left(\frac{R_i}{R_o}\right) \times \left(R \frac{\partial C'}{\partial R}\right)_{R=R_i} \quad (15)$$

$$Sh = \frac{1}{2f} \int_0^{2f} Sh_{\zeta} d\zeta. \quad (16)$$

3. Solution procedure

The governing equations were solved by using the finite volume technique developed by Patankar [15]. This technique was based on the discretization of the governing equations using the central differencing in space. Firstly the effect of the number of grids on the solution was examined. Fig. 2 shows the effect of number of grid on the solution. Through this study, the domain size was (92×72) used. A uniform grid distribution in both radial and circumferential directions was used. The discretization equations were solved by the Gauss–Seidel method. The iteration method used in this program is a line-by-line procedure, which is a combination of the direct method and the resulting Tri Diagonal Matrix Algorithm (TDMA). The convergence of the iteration is determined by the change in the average Nusselt and Sherwood numbers as well as other dependent variables through one hundred iterations to be less than 0.01% from its initial value. Fig. 3 shows the convergence and stability of the solution.

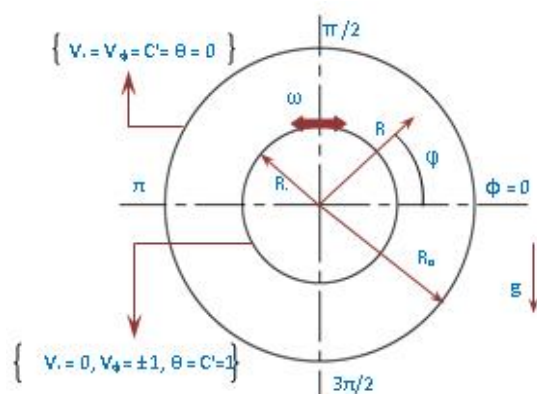


Figure 1. A Schematic Diagram of the Problem with Boundary Conditions

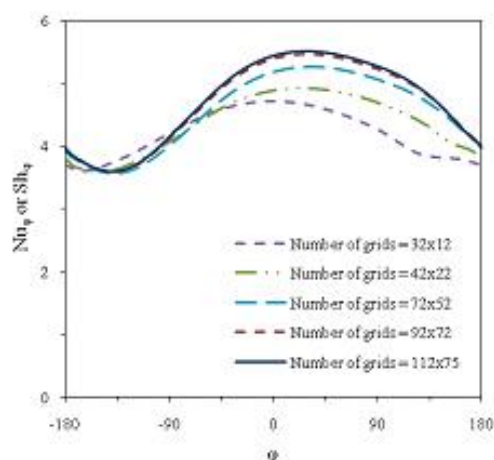


Figure 2. Convergence of the Local Nusselt and Sherwood Numbers at the Inner Cylinder for $Pr = 50$, $Le = 1$, $N = 1$ and $Ri = 1$

4. Program validation and comparison with previous work

The results reported by Mohamed A. Teamah [9] on double diffusion mixed convection of air in rotating annulus were used to benchmark them against the outcome of our program. Fig. 4 plots the average Nusselt number over a range of buoyancy ratio from -20 to 20 . Through the Fig., the thermal Rayleigh number was kept constant at 10^4 and rotational Reynolds number was kept constant at 100 . The Fig. shows a comparison between the results obtained from the program used in this investigation and the results published by Mohamed A. Teamah [9] for $Le = 1$ and $Le = 5$. The maximum deviation between the results was within 4%. In addition, the results are presented in Fig. 5 in terms of streamline and isotherm patterns where the inner cylinder was rotating in anti-

clockwise direction and the outer cylinder was kept constant. The dimensionless temperature and concentration at the inner cylinder were kept constant and their values equal unity while their values at the outer cylinder equal to zero. In addition, the Prandtl number was kept constant at 0.7. The value of Lewis number and Buoyancy ratio were kept constant and equaled unity. As shown in Fig. 5, the comparisons for $Ra_T = 10^3$ and 10^4 are in excellent agreements, which provide sufficient confidence in the numerical algorithm.

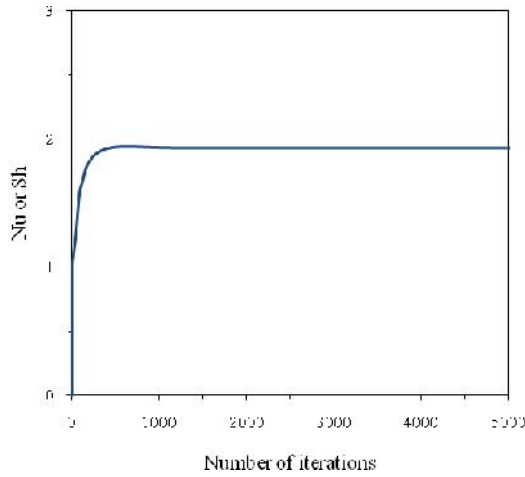


Figure 3. Average Nusselt and Sherwood Numbers $Pr = 0.7$, $Le = 1$, $N = 1$ and $Ri = 1$

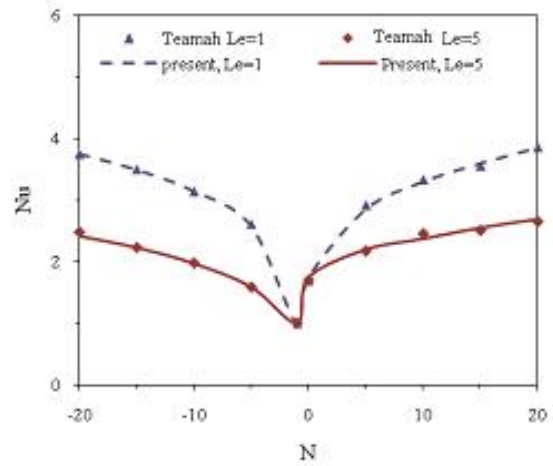


Figure 4. Comparison with Teamah [9], Anti-Clockwise Rotation, $Re = 100$, $Ra = 10^4$ and $Pr = 0.7$

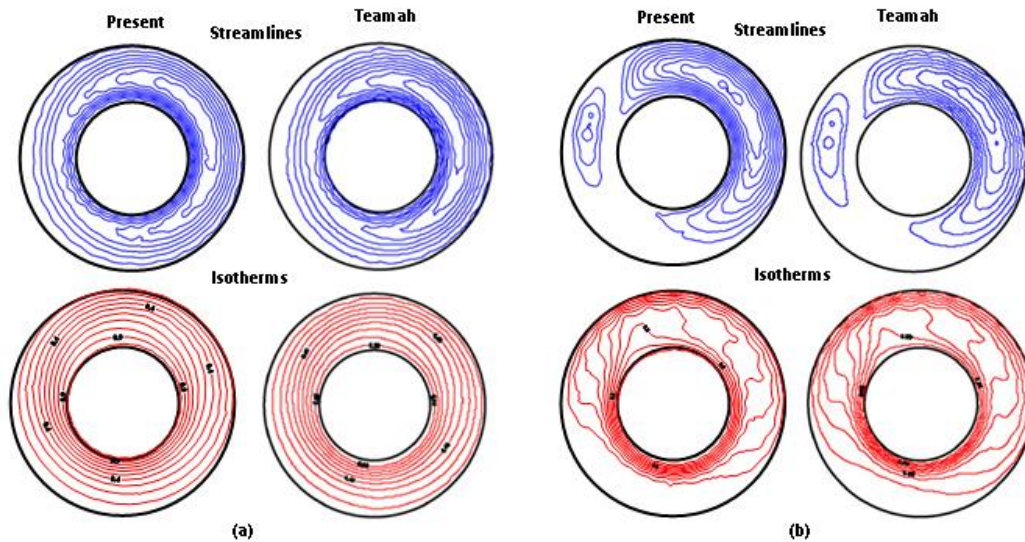


Figure 5. Comparisons of the Streamlines and Isotherms between the Present Work and Teamah [9] For $Pr = 0.7$, $N = 1$, $Le = 1$, $Re = 100$ and (a) $Ra_T = 10^3$, (b) $Ra_T = 10^4$

5. Results and discussion

Different scenarios were explored to explain the effects of different parameters on the studied problem. These two parameters are Prandtl number and buoyancy ratio. The results were obtained for the two cases of the inner cylinder rotation. The results were divided into local results and average results. Lewis number was kept constant at value equals one which means, the thermal diffusion equals the mass diffusion. Therefore, the isotherms are only presented. All results were performed with thermal Grashof number and radius ratio equaled to 10^4 and 2 respectively.

5.1. Effect of buoyancy ratio

a. The inner cylinder rotates in anti-clockwise direction

The effect of the Buoyancy ratio on the streamlines and isotherms for the anti-clockwise rotation is shown in Fig. 6 (a). At $N=-5$ the streamlines consist of two cells one at the right and the other one at the left portion of the annulus. The separation line is found to encompass the small eddy. As N is increased to -1 (the heat and mass diffusions are opposing each other), all eddies disappeared and the isotherms and streamlines are concentric circles around the inner cylinder and the flow looks like the couette flow pattern. Apparently, the forced convection has overwhelmed the diffusion behaviors in the annulus. As the buoyancy ratio equals to zero (mixed heat transfer dominated regime), the two eddies are found to form and the thermal plume is formed again but over the inner cylinder and tilted towards the left portion. In this case, the mass diffusion rate is no longer coupled with the velocity and the temperature fields since $\gamma_s = 0$, and hence, the problem reduces to a pure mixed thermal convection. At $N=1$, the heat and mass diffusions are adding to each other. Employing positive values of the buoyancy ratio causes a reversal in the basic flow pattern. They are showing reverse behaviors along the horizontal centerline of the annulus as compared to the negative values for the buoyancy ratio. The prediction of the effect of buoyancy ratio on both local Nusselt and Sherwood numbers is presented in Fig. 7(a). For $N = -1$, the values of both Local Nusselt and Sherwood numbers are fixed and equal to one. That means the conduction mode is dominated for both heat and mass transfer. As the buoyancy ratio departs from unity, the mixed convection pronounces and local values increase. For negative N values, the minimum points locate under the inner cylinder but the maximum points locate over the inner cylinder. This behavior is reversed for the positive N values. For positive and negative N values, the minimum points of the local Nusselt and Sherwood numbers move in the opposite direction of the cylinder rotation as the absolute value of N increases. Furthermore, as the absolute value of buoyancy ratio is increased the natural convection is dominated.

b. The inner cylinder rotates in clockwise direction

The effect of the Buoyancy ratio on the streamlines and isotherms for the clockwise rotation is shown in Fig. 6 (b). To explore the effect of buoyancy ratio, the thermal Grashof number is kept constant at 10^4 and the value of Lewis number equals to unity. The right cell is stronger than the left. Furthermore, the rotational speed drags the right cell downward and onto the left portion and pushes the right one upward. On the other hand, the thermal plume is noticed below the inner cylinder and tilted towards the left portion.

5.2. Effect of Prandtl number

The effect of Prandtl number on the streamlines and isotherms for the anti-clockwise rotation is shown in Fig.8 (a) and Fig. 8 (b) for clockwise direction. The streamlines consist of two cells, one at the right and the other at the left portion of the cavity. The right eddy is the stronger eddy where the left eddy is the weaker eddy. That is because; the forced flow is added to the buoyancy induced flow in the right portion but opposed the buoyancy induced flow in the left portion. At $Pr = 0.01$, the velocity gradient is very small so the streamline patterns strength is weak. As Prandtl increases, the viscous force increases then the flow pattern strength increases. At $Pr = 0.7$, the thermal and the momentum diffusion are almost equaled. The rotation effect becomes more

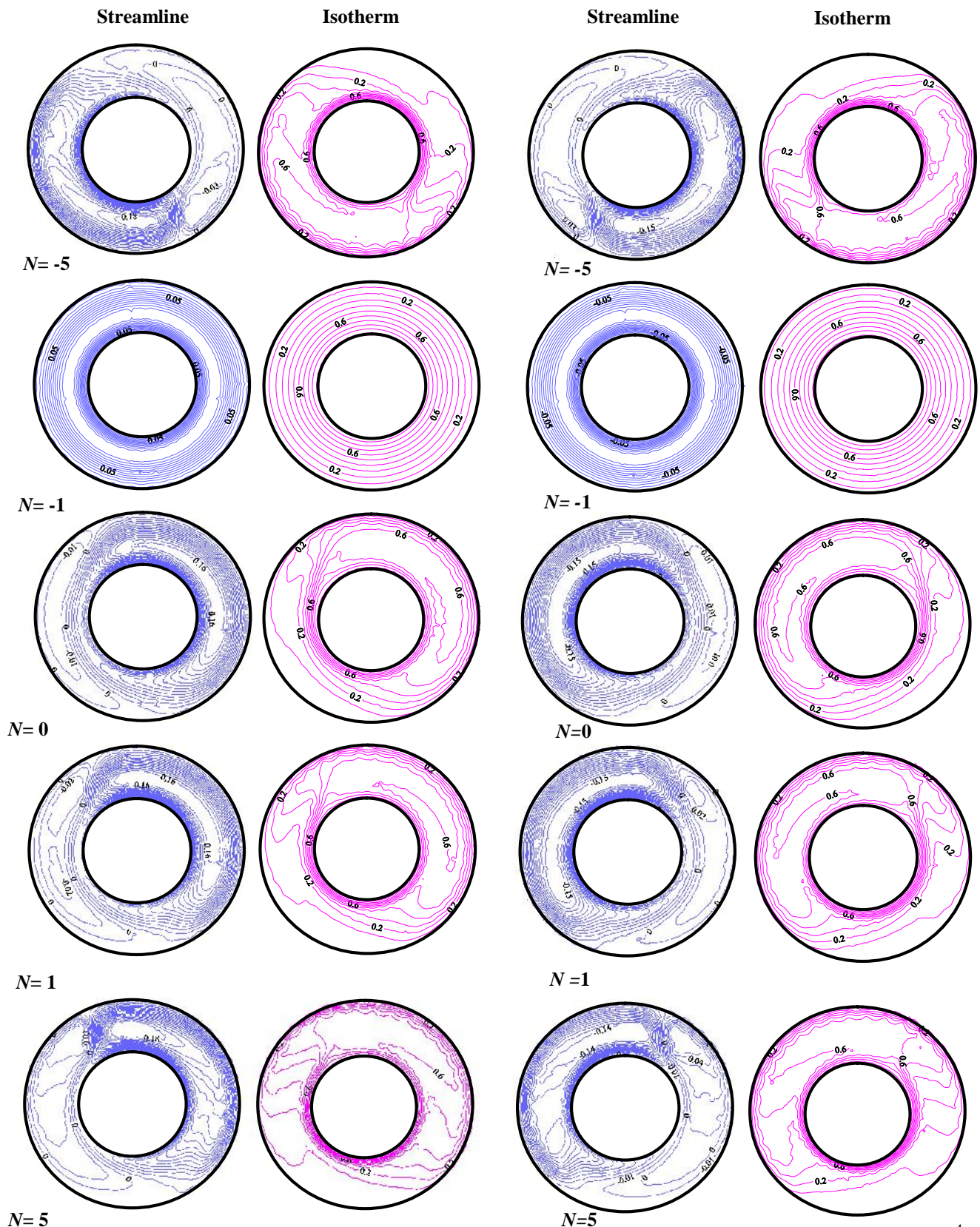


Figure 6. Effect of Buoyancy ratio on the Streamlines and Isotherms for $Le = 1$, $Ri = 1$, $Gr_T = 10^4$, $Pr = 6$ and (a) Inner Cylinder Rotates in Anti-Clockwise, (b) Inner Cylinder Rotates in Clockwise Direction

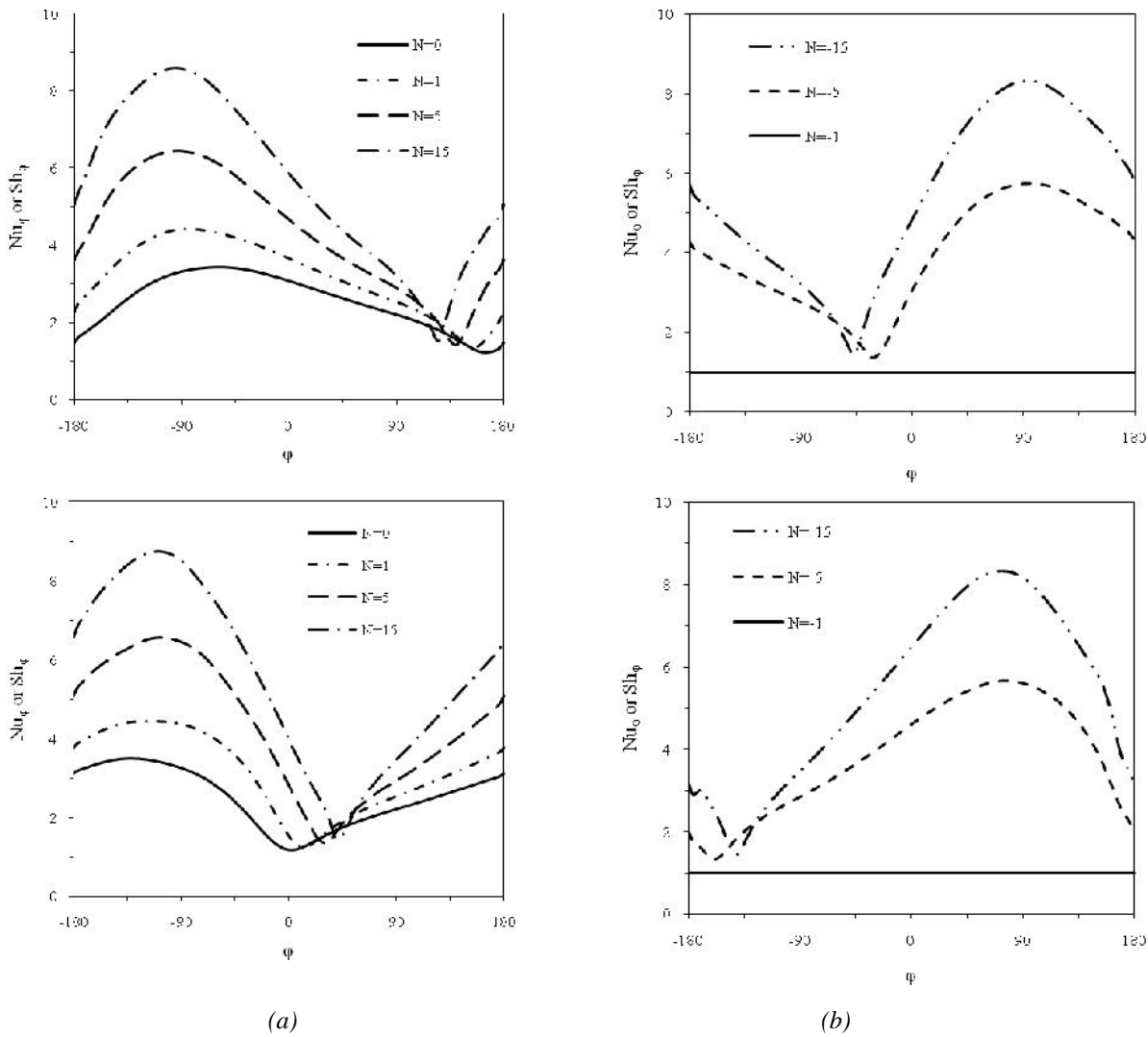


Figure 7. Effect of Buoyancy Ratio on the Local Nusselt and Sherwood Numbers for $Le = 1$, $Ri = 1$, $Gr_T = 10^4$, $Pr = 6$ (a) Inner Cylinder Rotates in Anti-Clockwise, (b) Inner Cylinder Rotates in Clockwise Direction

pronounced with the increase of Pr . that can be seen by the continuous growth of the large eddy and diminishing for the small eddy as Pr increases. As Pr increased to 6, the streamline of $\omega = 0.01$ also encompasses the small eddy which gets smaller. At $Pr = 100$, the small eddy disappears and the separation line encompasses the remaining eddy. The flow pattern moves from two eddies towards one eddy. The high viscous force causes the high velocity gradient so the flow pattern strength is relatively high. As for the isotherms, at $Pr = 0.01$, the thermal diffusivity is relatively high or the thermal conductivity of the given fluid is high and the thermal heating capacity is small then the thermal energy is conducted through all the fluid with almost the same rate since no energy is stored in the fluid so that the isotherms could be represented by a concentric circles. When Pr reaches 0.1, it can be seen that, the thermal plume starts to form at the top of the inner cylinder and the isotherms start to be close to each other at the bottom of the inner cylinder. At $Pr = 0.7$, the thermal plume gets bigger and tilted in the direction of the cylinder rotation. As Pr increases, the thermal plume moves in the direction of the cylinder rotation. At $Pr = 6$, the thermal plume increases in size. For this case, the thermal diffusivity decreases then the thermal heating capacity increases. As Prandtl increases, the thermal plume gets bigger and a gap space starts to form in the upper region of the annulus. At $Pr = 100$, the thermal heating capacity is very high then the thermal energy is transferred through a thin layer near the inner cylinder and most of the energy is absorbed through the fluid then no more energy will be available to be transferred through the rest of the fluid

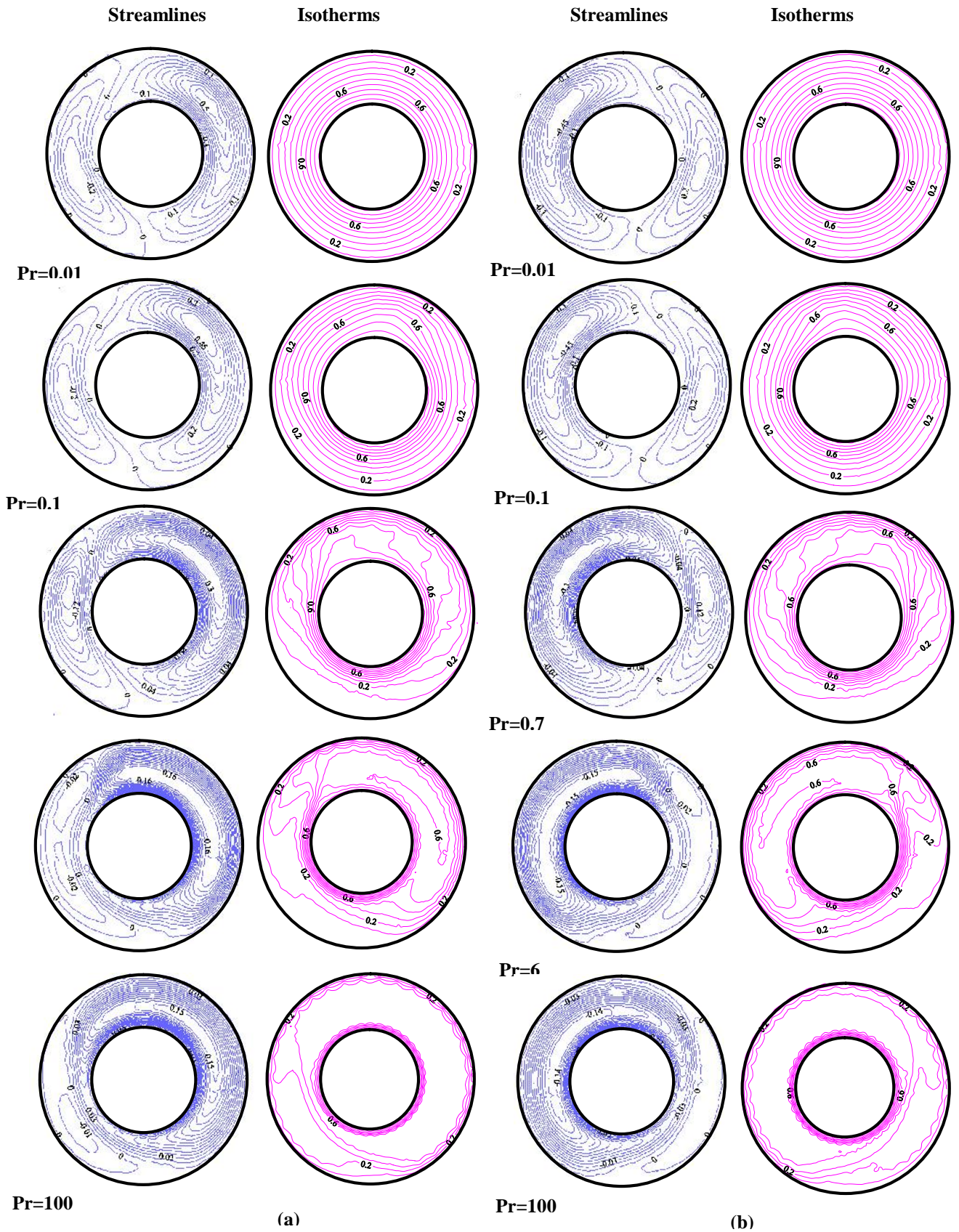


Figure 8. Effect of Prandtl Number on the Streamlines and Isotherms for $Le = 1$, $Ri = 1$, $Gr_T = 10^4$, $N=1$ and (a) Inner Cylinder Rotates in Anti-Clockwise, (b) Inner Cylinder Rotates in Clockwise Direction

so we can find a large gap space around the inner cylinder between the inner and outer isotherms. Fig. 9 presents the effect of the Richardson number on both average Nusselt and Sherwood numbers at different Prandtl number. The range of Richardson number was selected in the domain (0.01 Ri 100) to examined the three types of convection on the heat and mass transfer. Prandtl number values were selected to be 0.01, 0.7, 6.0 and 100 to exanimate all the fluid types and their behaviors. The results were obtained for $N = 1$, $Le = 1$ and $Gr_T = 10^4$ and it was denoted that for the liquid metals ($Pr = 0.01$), as Ri increased, the average Nusselt and Sherwood numbers are almost kept constant at value equals to unity. This is because the very small Pr value which makes the fluid conductivity is high and the heating capacity is small so the heat is transferred by the conduction mode then there is no effect of increasing the Reynolds number on the heat and mass transfer. As Pr increases (the case of mind fluid), there is a kind of competition between the buoyancy induced flow and the forced flow. At high Ri (dominated natural convection regime), there is no effect of increasing the cylinder rotation speed and the value of the average Nusselt and Sherwood numbers are kept constant. At low Ri (dominated mixed and forced convection regime), as the speed of the inner cylinder rotation increase, the average Nusselt and Sherwood numbers decreases rapidly. For heavy oils ($Pr = 100$), the momentum diffusion is 100 times the thermal and species diffusion then the speed of the inner cylinder rotation effects on the average Nusselt and Sherwood numbers value. At high Ri , the average Nusselt and Sherwood numbers are held at a constant value for a specific range of Ri . As Pr increases, this specific range decreases until Pr reaches 100, this specific range becomes smaller and the effect of the rotation velocity increases which cause a drop in the average Nusselt and Sherwood numbers value. For liquid metals and air, there is no difference between the two cylinder rotation directions. As Pr increases, the difference becomes pronounced and we can see that the clockwise rotation gives better heat and species transfer than the other direction.

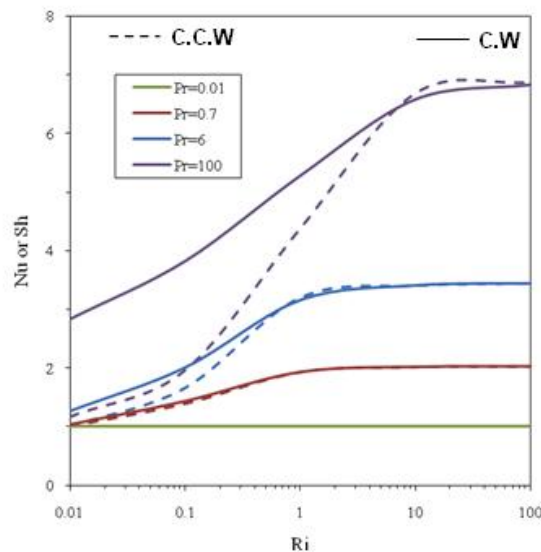


Figure 9. Combined Effect of Richardson Number and Prandtl Number on the Average Nusselt and Sherwood Numbers for $Le = 1$, $Gr_T = 10^4$ and $N = 1$

5.3 Combined effect of buoyancy ratio and Prandtl number

Figs. (10 and 11) present the effect of Buoyancy ratio on both average Nusselt and Sherwood numbers at different Prandtl numbers for the forced and mixed convection dominated regime. The range of the Buoyancy ratio is $-15 \leq N \leq 15$, Prandtl number values are 0.01, 0.7, 6 and 50. The results were obtained for $Gr_T = 10^4$, $Le = 1$ and $Ri = 1$ and 0.01. no pronounced effect can be detected for the Prandtl number on the effect of the direction of the inner cylinder rotation on heat

and mass transfer only when Prandtl reaches 50, the anti-clockwise gives higher heat and mass transfer than the clockwise rotation for both values of N and this behaviour is found when $Ri = 1$. But for the pure forced convection case ($Ri=0.01$, for $Pr = 0.01$, there is no difference between the clockwise and anti-clockwise rotation as there is no effect for the cylinder rotation on the heat and mass transfer in this case. At $Pr = 0.7$ and for positive N , the clockwise rotation gives better heat and mass transfer than the anti-clockwise rotation but for the negative N , we examined a reversal behaviour. As Pr increases this behaviour becomes more pronounced and the difference between the effect of the clockwise and anti-clockwise rotation on the heat and mass transfer increases. From the above, we can concluded that the direction of the inner cylinder rotation makes a difference when a forced convection heat and mass transfer is considered for the mind and heavy oil fluid but for the mixed convection case, the direction of the inner cylinder rotation makes a difference for the heavy oils only because of the very high value of Pr which makes the effect of the cylinder rotation high and consequently, the direction of the cylinder rotation.

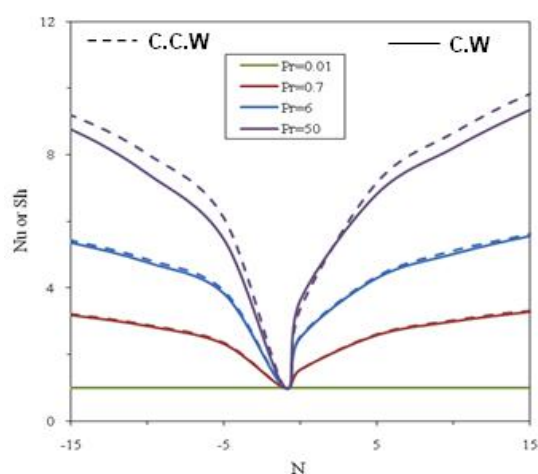


Figure 10. Combined Effect of Prandtl Number and Buoyancy Ratio on the Average Nusselt and Sherwood Numbers for $Le=1$, $Gr_T = 10^4$ and $Ri = 1$

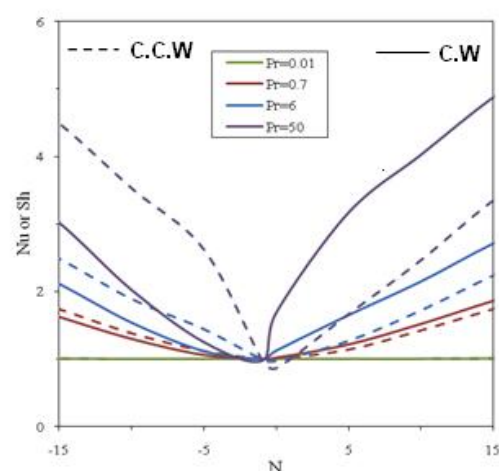


Figure 11. Combined Effect of Prandtl Number and buoyancy Ratio on the Average Nusselt and Sherwood Numbers for $Le = 1$, $Gr_T = 10^4$ and $Ri = 0.01$

6. Conclusion

The effect of the investigation parameters on the heat and mass transfer was studied and we can conclude that, the heat and mass transfer increased as Prandtl number and the absolute value of the buoyancy ratio increased. On the other hand, the effect of the direction of the inner cylinder rotation on the average Nusselt and Sherwood numbers becomes more pronounced at high values of the Prandtl and the buoyancy ratio. For all investigation ranges, and for the positive buoyancy ratio and as the Prandtl number increases, the clockwise rotation gives better heat and mass transfer compared with the other direction.

Nomenclature

b	annulus gab width $b=(r_o-r_i)$, m.
C	concentration.
C'	dimensionless vapour concentration.
C'_i, C'_o	dimensionless concentrations at inner and outer radii respectively.
D	mass diffusivity, m^2/s .
g	acceleration of gravity, m/s^2 .
Gr_s	solulal Grashof number based on the gab width.

Gr_T	thermal Grashof number based on the gap width.
h	heat transfer coefficient, $W/m^2 K$.
h_s	solubility transfer coefficient, m/s .
K	fluid thermal conductivity, $W/m K$.
Le	Lewis number, $Le = \nu/D$.
N	Buoyancy ratio.
Nu	average Nusselt number.
Nu	local Nusselt number.
P	pressure, N/m^2 .
P'	dimensionless pressure
Pr	Prandtl number.
r	radial coordinate.
r_i, r_o	inner and outer radii respectively, m
R	dimensionless radial coordinates.
Ri	Richardson number, $Ri = Gr/Re^2$.
Ras	solubility Rayleigh number based on the gap width.
Ra_T	thermal Rayleigh number based on the gap width.
Re	rotational Reynolds number.
Sc	Schmidt number.
Sh	average Sherwood number.
Sh	local Sherwood number.
T	local temperature, K .
T_i, T_o	temperatures at inner and outer radii respectively, K .
ΔT	temperature difference, $(T_i - T_o)$, K .
u	velocity vector, m/s .
U	dimensionless velocity vector.

Greek symbols

β_T	Coefficient of thermal expansion, K^{-1} .
β_s	Coefficient of solubility expansion, Kg^{-1} .
ν	Thermal diffusivity, m^2/s .
ϕ	angular coordinate
ω	angular velocity, rad/s .
ψ	dimensionless stream function
θ	dimensionless temperature.
ν	Kinematic viscosity, m^2/s .
ρ	Fluid density, Kg/m^3 .

References

- [1] Joo Sik Yoo, Natural convection in a narrow horizontal cylindrical annulus: $Pr = 0.3$, *Int. J. Heat Mass Transfer*, 41(1998), 3055-3073.
- [2] Joo Sik Yoo, Prandtl number effect on bifurcation and dual solutions in natural convection in a horizontal annulus, *Int. J. Heat Mass Transfer*, 42 (1999) 3279-3290.
- [3] Joo Sik Yoo, Dual free-convective flows in a horizontal annulus with a constant heat flux wall, *Int. J. Heat Mass Transfer*, 46 (2003) 2499–2503.
- [4] Jiro Mizushima, Sachiko Hayashi, Takahiro Adachi, Transitions of natural convection in a horizontal annulus, *Int. J. Heat Mass Transfer*, 44 (2001) 1249-1257.
- [5] E. M. Alawadhi, Natural convection flow in a horizontal annulus with an oscillating inner cylinder using Lagrangian–Eulerian kinematics, *Computers and Fluids*, 37(2008) 1253–1261.

- [6] C. Desai, K. Vafait, Experimental and numerical study of buoyancy induced flow and heat transfer in an open annular cavity, *Int. J. Heat Mass Transfer*, 39 (1996) 2053-2066.
- [7] M. Amoura , N. Zeraibi , A. Smati , M. Gareche, Finite element study of mixed convection for non-Newtonian fluid between two coaxial rotating cylinders, *Int. Comm. Heat Mass Transfer*, 33(2006) 780–789.
- [8] A. M. Al-Amiri, K. M. Khanafer, Numerical simulation of double-diffusive mixed convection within a rotating horizontal annulus, *Int. J. Thermal Sciences*, 45 (2006) 567–578.
- [9] M. A. Teamah, Numerical simulation of double diffusive laminar mixed convection in a horizontal annulus with hot, solutal and rotating inner cylinder, *Int. J. Thermal Sciences*, 46 (2007) 637–648.
- [10] J. Lee, S. H. Kang, Y. S. Son, Experimental study of double diffusive convection in a rotating annulus with lateral heating, *Int. J. Heat Mass Transfer*, 42(1999) 821-832.
- [11] M. Marcoux, M.C. Charrier –Mojtabi, M. Azaiez, Double diffusive convection in an annular vertical porous Layer, *Int. J. Heat Mass Transfer*, 42(1999) 2313-2325.
- [12] K. Khanafer, A. Al-Amiri, I. Pop, Numerical analysis of natural convection heat transfer in a horizontal annulus partially filled with a fluid-saturated porous substrate, *Int. J. Heat Mass Transfer*, 51(2008) 1613–1627.
- [13] S. Kenjeres, K. Hanjalic, Prediction of turbulent thermal convection in concentric and eccentric horizontal annuli, *Int. J. Heat Fluid Flow*, 16 (1995), 429-439.
- [14] M. Rahnama, M. Farhadi, Effect of radial fins on two-dimensional turbulent natural convection in a horizontal annulus, *Int. J. Thermal Sciences*, 43 (2004), 255–264.
- [15] S.V.Patankar, *Numerical Heat transfer and Fluid flow*, McGRAW-HILL, New York, 1980.